2021

Genetic Analysis of Cellular Adhesion in *Arabidopsis thaliana*

Andrew Close Bolender
Bowdoin College

Genetic Analysis of Cellular Adhesion in *Arabidopsis thaliana*

An Honors Paper for the Program of Biochemistry

By Andrew Close Bolender

Bowdoin College, 2021

TABLE OF CONTENTS

AKNOWLEDGMENTS

I would like to thank Bruce Kohorn for his guidance and support throughout this project. Despite the highly unusual campus environment this year, the unwavering dedication to mentorship, excitement for science, and quick wit he brought into the lab made this experience more rewarding than I could have ever imagined. Thank you to Sue Kohorn for her contagious positivity and enthusiasm, as well as her technical assistance and green thumb. I would also like to thank my reader, Stephanie Richards, for her thoughtful feedback during the writing process. Thank you to Wesley Hudson for his great sense of humor and lab discussions.

ABSTRACT

Plant cell adhesion is mediated by the extracellular matrix (ECM) or cell wall and plays an important role in plant morphogenesis and development. The amount, modification, and cleavage of pectin in the cell wall are major contributors to the adhesive properties of the ECM. To gain a more complete picture of plant cell adhesion processes, *Arabidopsis thaliana* seedlings were previously mutagenized and screened for hypocotyl adhesion defects. Genomic sequencing of one plant exhibiting an adhesion defect, isolate 242, showed that two mutations, one in cellulose synthase (CesA1) and another in a sugar transporter, are candidates for the causative mutation. This thesis reports that CesA1 is necessary for proper plant cell adhesion, while the sugar transporter encoded at At4g32390 is not. Dark grown seedlings homozygous for mutations in *CesA1* stain in ruthenium red, indicating atypical adhesion, while those homozygous for null mutations in At4g32390 do not. Previous study of another adhesion mutant revealed *ELMO1*, a Golgi protein necessary for plant cell adhesion, and four additional homologs ELMO2-5 in the *A. thaliana* genome. Two of these homologs, ELMO2 and ELMO3, fused to GFP, colocalized with mCherry-MEM1 markers in the Golgi, but not mCherry-NLM12 ER markers, indicating that ELMO2 and ELMO3 are also Golgi proteins.

INTRODUCTION

The regulation of adhesion between cells is a key process in plant morphogenesis and development. On the one hand, some cells stay positioned next to their neighbors in highly organized tissue for their entire lifetime (Knox 1992). On the other, many key processes in plant life strategy require the controlled separation of cells, such as organ abscission, dehiscence, and ripening (Daher and Braybrook 2015). Thus, plant cell adhesion requires a vast and dynamic regulatory framework. These complex adhesion processes are primarily mediated by the extracellular matrix (ECM), also called the cell wall (Jarvis et al. 2003). In plant cells, the ECM is divided into two regions: the primary cell wall, which lies directly outside the plasma membrane, and the middle lamella, which lies at the interface between the primary cell walls of adjacent cells (Höfte et al. 2012). The primary cell wall is thought to exhibit enough stiffness to support plant structural integrity while remaining flexible enough to accommodate cell growth and provides a scaffold for the secreted proteins involved in response to environmental stimuli and cell-to-cell signaling. The middle lamella is considered an adhesive layer between cells (Jarvis et al. 2003). When some plant cells stop growing, they develop a more rigid secondary cell wall between the plasma membrane and the primary cell wall, conferring even greater structural support in plant tissues (Endler and Persson 2011).

ECM architecture

In plant cells, the ECM structures underlying cellular adhesion arise during cell division such that daughter cells adhere upon formation (Fig. 1a) (Knox 1992; Jarvis et al. 2003). During cytokinesis, a cell plate is formed when Golgi-derived vesicles deposit a layer of pectin between dividing cells (van Oostende-Triplet et al. 2017; Miart et al. 2014). After this pectin gel-like

matrix expands to partition one daughter cell from another, cellulose, hemicellulose, and pectin are deposited by each cell to form a primary cell wall on either side of the pectin-rich plate, leaving the plate itself to become the middle lamella (Drakakaki 2015).

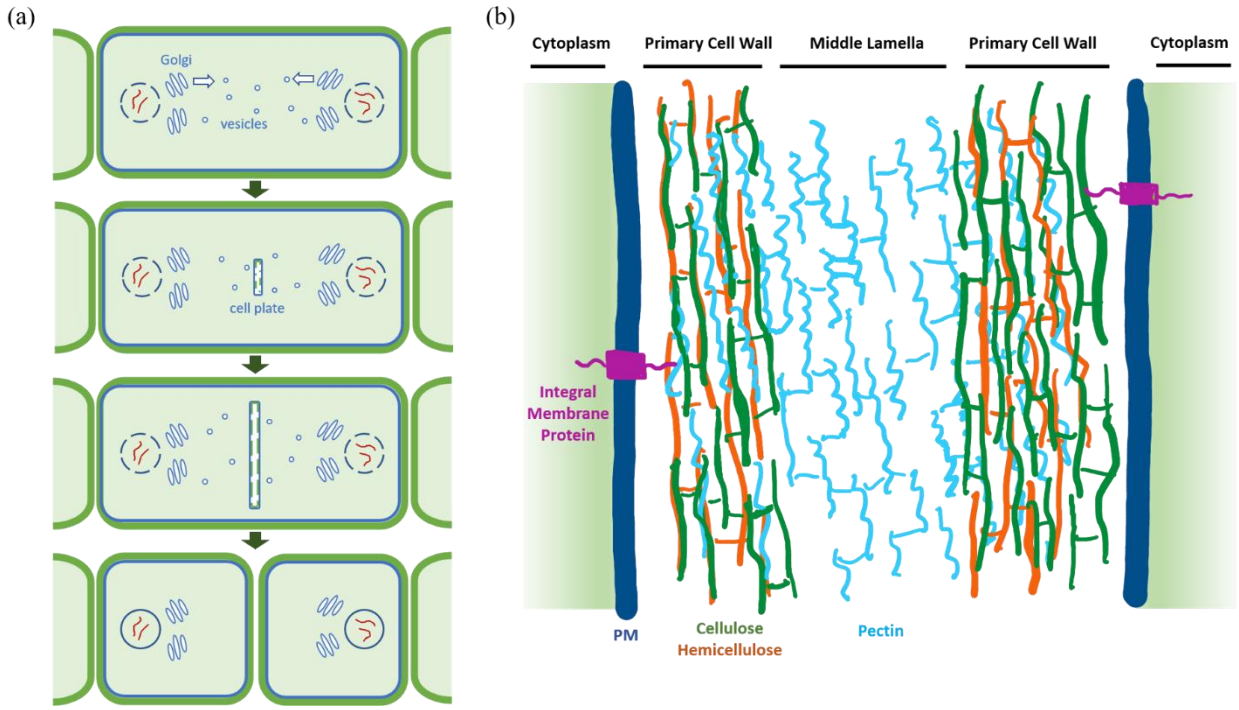

Figure 1. Architecture of the ECM. (a) Schematic representation of the formation of the ECM during cell division. (b) Schematic representation of key components of the ECM, with navy plasma membrane (PM), magenta integral membrane proteins, green cellulose, orange hemicellulose, and cyan pectin.

The primary cell wall is largely composed of cellulose, hemicellulose, and pectin, which work alongside a multitude of other embedded proteins and sugars to carry out its many functions (Fig. 1b). Cellulose is produced at the plasma membrane by large multimeric cellulose synthase complexes known as “rosettes” for their hexameric structure (Brown Jr and Chemistry 1996). Each rosette spans the plasma membrane and is composed of 6 globular complexes (Kimura et al. 1999). Traditionally, each of these lobes was thought to hold up to six CesA proteins, the catalytic subunits of cellulose synthase, on the cytoplasmic end of the rosette, though more recent studies suggest that each only holds three (Newman et al. 2013; Hill et al.

2014; Nixon et al. 2016; Vandavasi et al. 2016). The Arabidopsis CesA family is composed of 10 *CesA* genes. *CesA1, CesA2, CesA3, CesA5, CesA6, and CesA9* have been associated with cellulose synthase complexes active during primary wall formation (Arioli et al. 1998; Fagard et al. 2000; Scheible et al. 2001; Desprez et al. 2002; Persson et al. 2007b). Among these, *CesA1 and CesA3* are thought to have unique functions, as null mutations of each are embryonic lethal (Beeckman et al. 2002; Gillmor et al. 2002). During cellulose synthesis, each CesA present produces a single β-1,4 glucan chain simultaneously with the others, using UDP-glucose as a substrate. The length of each chain can range from 800-10,000 glycosyl subunits (Klemm et al. 2005). As they are synthesized, the chains are extruded toward the ECM, where they spontaneously self-assemble into crystalline microfibrils via hydrogen bonding and van der Walls forces (Nishiyama et al. 2002; Nishiyama et al. 2003). These microfibrils act as cables that contain the cell, impeding turgor-driven expansion along their parallel axes (Baskin 2005; Suslov and Verbelen 2006; Van Sandt et al. 2007).

Hemicellulose crosslinks to cellulose microfibrils via hydrogen bonds to mediate cellulose slippage, alignment, and separation during expansion (Daher and Braybrook 2015). Unlike cellulose, hemicellulose polymers are composed of a mixture of β-(1-4) glucose, mannose, and xylose and are often branched (Scheller and Ulvskov 2010). Hemicellulose synthesis occurs in the Golgi, where glycosyl transferases polymerize the polysaccharide backbone while acetyl transferases and acetyl-CoA acetylate the chains to varying degrees. (Pauly and Scheller 2000). The hemicellulose is then exported via vesicles to the plasma membrane, where it is secreted into the ECM. There, it undergoes trimming by glycosidases (Pauly et al. 2013). This cellulose-hemicellulose matrix is traditionally thought to be the primary load-bearing system in the ECM.

Pectins, while dominating the middle lamella, also play an important role in primary cell wall architecture. In fact, some studies suggest that the pectin matrix possesses a much greater load bearing capacity than held by the traditional view, and that the middle lamella may even be stronger than primary cell walls in certain cases (Zamil and Geitmann 2017; Kim et al. 2015; Höfte et al. 2012; Dick-Pérez et al. 2011). Pectins are largely synthesized in the Golgi and characterized by high levels of D-galaturonic acid. Plants have evolved over 60 enzymatic activities to synthesize different varieties of pectin, resulting in a variety of pectin forms within and between species (Atmodjo et al. 2013). Most common and conserved forms are homogalacturonan (HG), rhamnogalacturonan I and II (RG-I and -II), and xylogalacturonan (XG) (Ridley et al. 2001; Caffall and Mohnen 2009). RG-I's backbone is composed of alternating glacturonic acid and rhamnose residues accompanied by arabinogalactan and arabinan side chains (Atmodjo et al. 2013; Ridley et al. 2001). It accounts for 20-30% of total pectin in the ECM (Mohnen 2008). Certain RG-I sidechains have exhibited covalent bonding to cellulose *in vitro*, implicating RG-I in linking the pectin and cellulose/hemicellulose matrices (Zykwinska et al. 2005). Furthermore, removal of arabinan side chains in the ECM correlated with adhesion-defective phenotypes in *Nicotiana plumbaginfolia* meristem cells (Iwai et al. 2001). These findings suggest RG-I might play a significant role in adhesion through its interactions with the cellulose in the ECM.

RG-II and XG combined account for less than 10% of the plant ECM. RG-II possesses galacturonic acid backbone with complex sugar sidechains. RG-II dimerizes using borate diester crosslinks (Ridley et al. 2001) and the absence of this crosslinking is associated with decreased meristem cell adhesion (Iwai et al. 2002). One explanation might be the regulation of pore size in

the ECM by RG-II dimers, which may impact the rigidity of the pectin matrix (Fleischer et al. 1999).

XG also possesses a galacturonic acid backbone, though it is characterized by xylose side chains. The LM8 XG epitope is localized at cells undergoing detachment in several angiosperms, suggesting a role in plant cell separation pathways (Willats et al. 2004).

While studies of each of these types of pectin have revealed potential roles in cell adhesion, results largely emphasize the role of HG pectin. HG pectin is mostly conserved across land plants, but RG-I and RG-II side chains vary between species, while XG is not present in *Physcomitrella patens*, a widely used model organism in the study of plant evolution (McCarthy et al. 2014). These factors, alongside the prevalence of HG pectin relative to other types in the ECM, indicate that adhesion mechanisms surrounding these pectin types are likely less universal than those related to HG pectin.

HG pectin

HG pectin is the most abundant form of pectin in the ECM, accounting for 65% of pectin content (Mohnen 2008). As such, a large portion of plant cell adhesion research explores the synthesis and modification of HG pectin. A single HG pectin molecule is an unbranched, highly methyl-esterified chain of 100-200 α-(1-4)-linked D-galacturonic acid monomers (Mohnen 2008). The modification of these polymers plays a key role in their capacity to associate and form the gel-like matrix between adjacent cells. In a process that facilitates firmer adhesion between cells, calcium ions in the middle lamella are able to associate with newly freed negatively charged oxygens in the carbon-6 carboxyl groups of demethylesterified pectin backbone monomers (Braccini and Pérez 2001). The cross-linking of a pectin chain to a calcium

ion to another pectin links elements of the matrix spanning the ECM with strong ionic interactions, giving rise to a stiffer pectin matrix and stronger adhesion between cells.

HG synthesis begins in the Golgi. Glycosyl transferases, such as QUASIMODO1 (QUA1), facilitate polymerization of galacturonic acid subunits (Bouton et al. 2002) and methyltransferases, including QUA2, are thought to methylesterify the carboxyl group on carbon 6 of polymerizing HG pectin subunits (Mouille et al. 2007). QUA2 methyltransferase activity was recently confirmed *in vitro* using demethylesterified HG pectin as a substrate (Du et al. 2020). Highly methylesterified HG pectin is packaged in vesicles and exported to the plasma membrane for secretion into the ECM (Cosgrove 1997). Studies support the involvement of both actin-myosin microfilament and kinesin movement along microtubule systems in pectin secretion (Toyooka et al. 2009; Kim and Brandizzi 2014; Zhu et al. 2015).

The modification of pectin chains in the ECM adds a layer of complexity to the understanding of adhesion pathways. After secretion into the ECM, highly methylesterified HG pectin is demethylesterified by pectin methylesterases (PMEs) (Daher and Braybrook 2015; Micheli 2001). PME activity is associated with both increased and decreased levels of cell adhesion depending on tissue type. For example, higher levels of methylesterification as a result of low PME activity are associated with increased adhesion in tetraspores and root border cells while also correlating with decreased adhesion in the mesophyll and pericarp (Tieman and Handa 1994; Lionetti et al. 2015; Wen et al. 1999; Rhee et al. 2003). These differing effects can be explained by the varying activities of PMEs.

PME activity may loosen adhesion by making pectin susceptible to polygalacturonases (PGs), which cleave de-esterified pectins. Loss-of-function mutations in *QUARTET1 (QRT1)* and *QRT3,* which encode a PME and PG respectively, each result in tetraspore separation defects

(Rhee et al. 2003; Francis et al. 2006). This phenotype implies that PME and PG activity are both required for tetraspore separation, where QRT1 demethyesterifies pectin and QRT3 subsequently cleaves it, loosening the pectin matrix and reducing local adhesion. Thus, demethylesterification by PMEs can result in increases or decreases in cellular adhesion, depending on the presence of calcium ions or PGs.

The expression of differently functioning PMEs may offer plant cells another method of tuning adhesion strength. The *A. thaliana* PME family includes 66 proteins (Tian et al. 2006). Different PMEs exhibit different patterns of demethylesterification. Some PMEs remove methyl groups in a linear or block-wise fashion along a given pectin chain, making many consecutive free oxygens available, while others do so in a more random, non-block-wise fashion (Daher and Braybrook 2015). Some PME isoforms act linearly at alkaline pH and randomly at acidic pH (Micheli 2001). Block-wise demethylesterification is thought to be more effective at facilitating calcium crosslinking, and is associated with pectin-gel stiffening and increased adhesion. Preferentially expressing linear PMEs might encourage stiffer adhesion over expression of random PMEs, which might offer a mechanism for plants to achieve threshold levels of pectin demethylesterification necessary to initiate other pathways (like PG activity) while minimizing calcium crosslinking.

Furthermore, pectin demethylesterification is controlled by a wide host of regulation mechanisms. Solution pH and salt abundance have been shown to influence PME activity (Alonso et al. 1997; Denès et al. 2000; Jolie et al. 2010). PMEs can also be regulated by hormones, though the identities and effects of regulator hormones vary between species (Micheli 2001; Downie et al. 1998; Ren and Kermode 2000).

Pectin methyleseterase inhibitors (PMEIs) introduce another layer of regulation of the demethylesterification activity of PMEs. The Arabidopsis PMEI family contains 75 isoforms. PMEIs are themselves highly regulated transcriptionally (Nguyen et al. 2017; Srivastava et al. 2012; Lionetti et al. 2017; Hong et al. 2010), translationally (Rocchi et al. 2012), and by endocytic internalization from the ECM (Röckel et al. 2008). Overexpression of the Arabidopsis PMEIs AtPMEI-1 and AtPMEI-2 increased the efficiency of protoplast isolation from leaf mesophyll tissue, suggesting that adhesion was loosened to allow for the easier separation of cells (Lionetti et al. 2015). Some interactions between PMEs and PMEIs are pH dependent (Micheli 2001).

An association between aberrant pectin synthesis and adhesion defects supports a role for HG pectin in plant cell adhesion. *A. thaliana* mutants *qua1* and *qua2* reduce HG pectin content by 50% while exhibiting defective cell adhesion phenotypes such as detaching or "peeling" hypocotyl cells (Bouton et al. 2002; Mouille et al. 2007). These results suggest that HG pectin abundance is necessary for proper cell adhesion.

Pectin must not just be present, but also properly modified: Loss of function of a Golgi-localized putative *O*-fucosyl transferase encoded by *FRIABLE1* (*FRB1)* does not alter HG pectin abundance compared to wild type plants but does alter the methylation level of HG pectin and disrupts cellular adhesion, producing plants with sloughing cells that caused tissues to crumble (Neumetzler et al. 2012). This result indicates that proper regulation of methyesterification levels in pectin in the ECM is necessary for adhesion. PMEs might offer some explanation for *frb1* phenotypes: a PME was shown to be upregulated in the *frb1* mutant, which may have allowed for processes like PG activity to be carried out to loosen the middle lamella (Neumetzler et al. 2012).

Taken together, the regulatory framework described above reflects a complex and dynamic system for modulating the availability of demethylesterified HG pectin for calcium crosslinking to control the level of adhesion between plant cells.

Adhesion regulation beyond pectin availability

While the distribution of HG pectin and its modification in the ECM may carry a key role in plant cell adhesion, characterization of other mutants has revealed that additional factors are likely at play.

Low pectin levels do not universally preclude cellular adhesion. While the *irregular xylem8 (irx8)* mutant exhibits reduced xylan and homogalacturonan content, it produces dwarf but not adhesion-defective plants, indicating that scarcity of pectin molecules can be overcome to achieve adhesion (Persson et al. 2007a).

Recent work by the Kohorn lab identified a Golgi-localized protein, ELMO1, as essential for cellular adhesion in *A. thaliana,* and may be involved in mannose modification of ECM components (Kohorn et al. 2021b). As well as lowered mannose levels, *elmo1* mutants demonstrate similar phenotypes to *qua1* and *qua2* mutants, but of decreased severity, which may be accounted for by four additional *ELMO1* homologs that could provide redundancy in the *A. thaliana* genome (Kohorn et al. 2021b). ELMO1 has no predicted active sites, suggesting that it might act as a scaffold for other as yet undefined proteins in adhesion signaling pathways. Mannose has not previously been implicated in cellular adhesion pathways, and its role requires further study.

Furthermore, recent findings suggest that adhesion is likely controlled by an undefined signaling pathway. Mutations in *ESMERALDA1 (ESMD1),* which encodes a Golgi-localized

putative O-fucosyl transferase, suppress the pectin deficient *qua2* adhesion-defective phenotype but do not restore pectin levels (Verger et al. 2016). *qua2-1* and *frb1-2* single mutants each exhibit adhesion defects, while the double mutant *qua2-1/frb1-2* demonstrated non-additive adhesion defects, indicating that QUA2 and FRB1 operate in the same adhesion pathway (Verger et al. 2016). Mutations of *ESMD1* were shown to restore adhesion in *esmd1*$^{-/-}$*frb1*$^{-/-}$ double mutant and *esmd1*$^{-/-}$*qua2-1*$^{-/-}$ *frb1*$^{-/-}$ triple mutant plants (Verger et al. 2016). Recent work by the Kohorn lab demonstrated that *esmd1* also suppresses the *elmo1* adhesion defects (Kohorn et al. 2021b). These results indicate that QUA2, FRB1, ELMO1, and ESMD1 are affected by an as yet undefined signaling pathway regulating adhesion.

ESMD1 shares motifs with members of the fucosyltransferase superfamily, as well as the GDP-fucose protein *O*-fucosyltransferase signature, suggesting that the protein it targets for fucosylation contains either Epidermal growth factor (EGF)-like repeats or Thrombospondin type 1 repeats (TSRs) (Hansen et al. 2012; Wang et al. 2001; Verger et al. 2016). While no known *A. thaliana* proteins contain TSR domains, there are those that possess EGF-like repeats (Verger et al. 2016). Among these proteins, a smaller subset containing Wall Associated Kinases (WAKs) and S-locus receptor kinases (SRKs), both of which span the plasma membrane, possess conserved *O*-fucosylation sites within EGF-like domains. Between these two families, the fact that WAKs are ECM-associated while SRKs are not suggests that WAKs are a more likely substrate for ESMD1 in an adhesion signaling pathway (Takasaki et al. 2000; Cabrillac et al. 2001; Dwyer et al. 1994; Pastuglia et al. 1997). Mutation of the putative EGF substrate in WAKs and analysis in esmd1 mutants support this idea (Kohorn et al 2021a).

ECM signaling

The *A. thaliana* WAK family is comprised of 5 proteins, each with an EGF-repeat-containing extra cellular domain (65% conserved) that binds pectin in the ECM and a kinase intracellular domain (85% conserved), granting them the potential to transmit signals from the ECM to the cytoplasm (He et al. 1999; Wagner and Kohorn 2001; Kohorn and Kohorn 2012, Kohorn 2016). Under normal conditions, where native pectin binds to the extracellular domain, WAK function has been implicated in cell growth pathways. Leaves expressing a WAK antisense mutation exhibit dysfunctional leaf expansion (Lally et al. 2001; Wagner and Kohorn 2001). WAK2 mutations have also produced shortened roots and reduced expression and activity of vacuolar invertase, which plays an essential role in maintaining turgor pressure necessary for cell expansion (Kohorn et al. 2006).

While WAKs are associated with cell growth during normal conditions, they serve a dual function as a key player during stress response. Should wounding or pathogen presentation generate oligogalaturonides (OGs), pectin fragments, WAKs will preferentially bind to OGs over native pectin, resulting in a stress response (Decreux and Messiaen 2005; Decreux et al. 2006; Kohorn et al. 2006; Kohorn et al. 2009; Kohorn 2016). An overactive dominant allele of *WAK2*, *WAK2CTAP*, exhibits a pathogen response without the presence of a pathogen (Kohorn et al. 2009; Kohorn and Kohorn 2012; Kohorn 2016). When mutations were introduced into the *WAK2CTAP* pectin binding domain, EGF region, or catalytic kinase site, *WAK2CTAP* plants no longer exhibited the stress response, indicating that each functional part of the WAK2 receptor was necessary. This result supports the idea that WAK stress response requires active receptor function. How WAKs distinguish between OGs and native pectin for preferential binding

remains unknown, but it has been proposed that a competition between higher affinity OGs and native pectin pays a role (Kohorn 2016, 2015).

WAKs have not been directly implicated in adhesion pathways, but the fact that they possess the structural motifs necessary for interaction with fucosyl transferases like ESMD1 and are implicated in signal transduction from pectin in the ECM make them a potential route for further study.

In addition to the WAKs, the Feronia receptor kinase is another likely candidate for ECM and specifically pectin signaling. While Feronia is not thought to be involved in cell-cell adhesion, Feronia-regulated multiple developmental events from synergid fusion in fertilization to mechanosensing properties in leaf expansion have been documented (Ji et al. 2020). During pollination, pectin fragments from pollen tube growth may trigger Feronia-dependent nitric oxide accumulation in the filiform apparatus, inhibiting the LURE chemoattractants that would otherwise guide additional pollen tubes to the female gametophyte (Ji et al. 2020). Feronia may also interact with pectin at the PM-ECM interface to positively regulate levels of de-eseterified ovular pectin, stabilizing the pectin matrix to prevent polyspermy via multiple pollen tube entry (Ji et al. 2020). These potential ECM interactions suggest that Feronia is another candidate for further study of pectin signaling pathways.

Research objectives

The complexity of adhesion regulation and the suggestion of an unknown signaling pathway indicate that there is much to discover about cellular adhesion processes. In order to characterize the proteins involved in cell adhesion pathways, the Kohorn lab generated multiple adhesion-defective *A. thaliana* lines through EMS mutagenesis. Genomic sequencing identified

loci that when mutant affect cell adhesion. One adhesion mutant line under investigation is line 242, which exhibits RR staining and stunted root and hypocotyl growth. Among the candidate causal mutations for the adhesion defect revealed by sequencing, two emerged as high-priority for further investigation due to their potential to meaningfully alter protein expression or function: a mutation in locus At4g32390 that predicts a missense mutation Pro77Leu in the encoded Golgi sugar transporter and the alteration of a splice junction of *CesA1*, which encodes one of the catalytic subunits primary cell wall cellulose synthase. Using T-DNA insertion lines to generate single mutants with loss-of-function alleles for either the sugar transporter or *CesA1*, I investigated the potential roles of the sugar transporter mutation or the *CesA1* mutation as the sole cause of the adhesion-defective phenotype. The results indicated that *CesA1,* and not the sugar transporter is essential for cellular adhesion. Additionally, further characterize the ELMO family and the potential roles of its members in adhesion, I investigated the subcellular localization of two ELMO1 homologs in the *A. thaliana g*enome. GFP fusion experiments indicated that ELMO2 and ELMO3, like ELMO1, are Golgi proteins.

METHODS

Plant Growth

A. thaliana seeds were sterilized for 5 min in 95% ethanol, followed by 5 min in 10% bleach, before being rinsed twice in sterile dH_2O. Seeds were then plated in Murashige and Skoog (MS) liquid media (1X MS pH 5, 1% sucrose, 1X Vitamins, 50 ug/ml ampicillin) or MS agar (1X MS pH 5, 1% sucrose, 2% agarose, 1X Vitamins, 50 ug/ml ampicillin). Seeds in liquid media were stored at 4℃ for 48 hours, then exposed to light for 4 hours at 20℃ before being

grown at 20℃ in darkness for 4 days. Seeds plated on agar were stored at 4℃ for 48 hours, then grown in light at 20℃ for 2 weeks.

Adhesion screening

Dark-grown seedlings in liquid media were stained with Ruthenium Red (RR) dye as follows: Liquid media was removed and 3 ml RR dye (Sigma Corp., 0.5 mg/ml in dH_2O) was added for 2 min then seedlings were washed twice with 5 ml dH_2O, then observed under a dissecting microscope.

DNA extraction from leaves

Leaves were frozen in liquid nitrogen, then ground and homogenized by pestle in 400 µl DNA extraction buffer (1 M Tris pH 7.5, 5 M NaCl, 0.5 M EDTA, 10% SDS in dH_2O). Samples were centrifuged at 20,000 x g for 3 min. An equivalent volume of isopropanol was added to the supernatant and incubated at 25℃ for 10-15 min, then centrifuged at 20,000 x g for 5 min. The supernatant was discarded, and the pellet was washed with 400 µl 70% ethanol before centrifuging at 20,000 x g for 1 min. The supernatant was removed, then samples were centrifuged again at 20,000 x g for 1 min. The supernatant was again removed, and the pellets were left to air dry for 20 min before resuspension in 100 µl dH_2O and storage at -20℃.

PCR

PCR amplification of At4g32390 alleles used 1 µl extracted leaf DNA per 25 µl reaction in Titanium PCR mix (1X Titanium TAQ buffer (Takara Bio, Mnt View Ca.), 0.2 µM forward primer, 0.2 µM reverse primer, 0.1 mM dNTP mix, 0.5 µl Titanium TAQ Polymerase (Takara

Bio, Mnt View Ca.)) and was run under the following conditions: 1 min at 95℃, then 30 cycles of 30 sec at 95℃, 20 sec at 58℃, and 1 min at 68℃, followed by 1 min at 68℃ and hold at 4℃. See Table 1 for primers.

PCR amplification of *ELMO2* and *ELMO3* used 1 µl extracted leaf DNA from Col 0 plants per 25 µl reaction in Platinum SuperFi Polymerase mix (1X SuperFi buffer (Thermo Fisher), 0.2 mM dNTP mix, 0.5 µM forward primer, 0.5 µM reverse primer, 0.02 U/µl Platinum SuperFi Polymerase (Thermo Fisher)) and was run under the following conditions: 30 sec at 98℃, 30 cycles of 8 sec at 98℃, 10 sec at 58℃, and 1 min at 72℃, followed by 5 min at 72℃ and hold at 4℃. See Table 1 for primers.

Table 1. Primers used for PCR.

PCR Target	Forward Primer	Reverse Primer
At4g32390 WT Allele	5’-GCTACATTAGACAGACTCTCTCACACCAAAAG-3’ (AT4G32390F)	5’-CTGAATCAAAACCAACCTCGTTGCTTCG -3’ (AT4G32390R)
SALK_108775 Insert	5’-GCTACATTAGACAGACTCTCTCACACCAAAAG-3’ (AT4G32390F)	5’-ATTTTGCCGATTTCGGAAC-3’ (LBb1.3)
SALK_089917C Insert	5’-ATTTTGCCGATTTCGGAAC-3’ (LBb1.3)	5’-CTGAATCAAAACCAACCTCGTTGCTTCG -3’ (AT4G32390R)
ELMO2 cloning insert	5’-CCATGGCGAGACACACGGC-3’ (ELMO2NCOF)	5’-ACTAGTAGCAACCTGAACATTGCTTTTGGA-3’ (ELMO2SPER)
ELMO3 cloning insert	5’-CCATGACCAGAAGGCAGAAGAAGA C-3’ (ELMO3NCOF)	5’-AGATCTGCGATAACATCAGAAGCAACAGTTCCTTC-3’ (ELMO3BGLR2)

Gel electrophoresis

A mixture of 1% m/v agarose in 1X TAE (0.04 M Tris-acetate buffer and 0.001 M EDTA) was heated in a microwave for 90 seconds, then partially cooled. For a gel containing 75 ml 1X TAE, 5 µl 10 mg/ml ethidium bromide was added to the gel before it was poured into a gel plate. Loading dye was added to each sample to a final concentration of 1X, then samples were added to the gel. Gels were run at 130 V for 40-50 min.

Gel extraction and sequencing

Extraction of a PCR bands for the SALK_089917C, *ELMO2*, and *ELMO3* inserts was performed using the QIAquick gel extraction kit (Qiagen) according to manufacturer's instructions. Purified SALK_089917C PCR product was sequenced by Retrogen using primers LBb1.3 and AT4G32390R.

Cloning

Cloning into and transformation with pSC-A was performed using the StrataClone PCR Cloning Kit (Agilent) according to manufacturer instructions.

Ligation of sticky-ended *ELMO2* and *ELMO3* inserts isolated from pSC-A digests into restriction enzyme digested pCambia1302 (see "Plasmid digest") was performed using T4 DNA ligase (NEB) according to manufacturer instructions. Ligation reaction mix was added to DH5-α *E. coli.* Cells were incubated on ice for 30 min, heat shocked for 45 sec at 42°C, then put on ice for 2 min. 1 ml LB broth was added to cells. Cells were incubated for 1 hr at 37°C, then centrifuged for 3 min at 6000 xg. The cell pellet was resuspended in 100 µl LB, and the suspension was plated on LB kanamycin (Kan) agar. Plates were incubated for 12-16 hr at 37°C.

Plasmid preparation

White colonies of StrataClone competent cells transformed with pSC-A (see "Cloning") were picked, added to 1.5 ml LB ampicillin, and incubated in an orbital shaker at 37℃ for 12-16 hr.

Colonies of DH5-α competent cells transformed with pCambia1302 (see "Cloning") were picked, added to 1.5 ml LB Kan, and incubated in an orbital shaker at 37℃ for 12-16 hr.

In all cases, approximately 100 µl cell suspension was set aside as a stock culture. Remaining cells were pelleted at 6000 xg for 3 min at 4℃, and supernatant was removed. The pellet was resuspended in ice cold resuspension solution (50 mM glucose, 25 mM Tris-Cl (pH 8.0), 10 mM EDTA (pH 8.0) in H_2O). Two volumes lysis solution (0.2 N NaOH, 1% SDS in H_2O) to one volume resuspension solution was added. Samples were mixed by gentle inversion and incubated at room temperature for 5 mins. 1.5 volumes ice cold neutralization solution (3 M potassium, 5 M acetate in H_2O) to one volume resuspension buffer was added. Samples were mixed by gentle inversion, incubated on ice for 5 mins, then centrifuged at 12,000 xg for 5 min at 4℃. The supernatant was transferred to a new tube, and 0.6 volume isopropanol was added to the supernatant. Samples were mixed by inversion, incubated at room temperature for 5 min, then centrifuged at 12,000 xg for 5 min at 4℃. The supernatant was discarded and the pellet was washed in 70% EtOH. Samples were centrifuged at 13,000 xg for 5 min at 4℃, supernatant was discarded, and pellets were allowed to dry before being resuspended in 40 µl H_2O.

Cloned pCambia1302 was purified from DH5-α cultures confirmed to contain transformants (see "Plasmid digest") using the Monarch Plasmid Miniprep Kit (NEB) according to manufacturer instruction.

Plasmid digest

Isolated pSC-A cloned with *ELMO2* insert, uncloned pCambia1302 for subsequent *ELMO2* insert cloning, and isolated pCambia1302 cloned with *ELMO2* insert (see "Plasmid preparation") were digested with NcoI-HF (NEB) and SpeI-HF (NEB) according to manufacturer instructions.

Isolated pSC-A cloned with *ELMO3* insert, pCambia1302 for subsequent *ELMO3* insert cloning, and isolated pCambia1302 cloned with *ELMO3* insert (see "Plasmid preparation") were digested with NcoI (NEB) and BglII (NEB) according to manufacturer instructions.

Gel electrophoresis was performed on digests of cloned plasmid to confirm the presence of *ELMO* inserts (see "Gel electrophoresis"). Insert bands from pSC-A digests were extracted using the Qiaquick Gel Extraction Kit (Qiagen) according to manufacturer instructions. Uncloned pCambia1302 digests were incubated for 10 min at 65°C to inactivate restriction enzymes for subsequent ligation reactions.

Protoplast isolation

Protoplasts from Wave line *A. thaliana* seed stocks CS781684 (ATMEMB12 At5G50440 Golgi) and CS781671 (AT-NLM1 NOD26-like intrinsic protein1 ER/plasma membrane) expressing sub-cellular markers were obtained from ABRC as described in Geldner et al. (2009). Approximately 10 fresh-cut leaves from plants of a Wave line were cut into thin strips. Vacuum was applied to leaf strips in enzyme+ solution (1% (w/v) cellulase, 0.2% (w/v) macerozyme, 0.009 M $CaCl_2$, 0.1% BSA (fraction V)(w/v), 0.4 M mannitol, 20 mM KCl, 20 mM MES (pH 5.7)) for 5 mins. Strips were shaken at 40 rpm for 1.5 hours, then 80 rpm for 1 min on orbital shaker. The mixture was gently filtered through 200 µm nylon mesh, and the

filtrate was centrifuged at 100 xg for 2 min. The supernatant was removed, the pellet was resuspended in 5 ml ice cold W5 solution (154 mM NaCl, 123 mM $CaCl_2$, 5 mM KCl, 2 mM MES (pH 5.7) was added, and the suspension was centrifuged at 100 xg for 2 min. The supernatant was removed, the pellet was resuspended in 5 ml ice cold W5. The suspension was incubated on ice for 30 min, then centrifuged at 100 xg for 2 min. The supernatant was removed and the pellet was resuspended in Mmg solution (0.4 M mannitol, 15 mM $MgCl_2$, 4 mM MES (pH5.7)) to a concentration of 1-2 x 10^5 ml^{-1}.

Protoplast transformation

Cloned pCambia1302 preparation (see "Cloning" and "Alkaline lysis") with 10 µg DNA, 100 µl isolated protoplasts (see "Protoplast isolation"), and 110 µl PEG solution (40% PEG4000 (w/v), 0.2 M mannitol, 90 mM $Ca(NO_3)_2$ in H_2O) were combined, mixed gently by inversion, and incubated at room temperature for 30 min. 440 µl room temperature W5 solution was added, and the samples were mixed by inversion before centrifugation at 100 xg for 3 min. Supernatant was removed, and the pellet was resuspended in 1.0 ml room temperature W5 before incubation at room temperature under direct light for 12-16 hours.

Transformed protoplasts were visualized on the Leica SP8 microscope. GFP, mCherry fusion proteins, and chlorophyll were detected by sequential scanning at the following wavelengths. GFP: excitation 488 nm, emission 510 nm. mCherry: excitation 587 nm, emission 610 nm. Chlorophyll: excitation 488 nm, emission 687 nm.

RESULTS

Mutant line 242 carries two high-priority mutations

To characterize essential genes for plant cellular adhesion, *A. thaliana* lines exhibiting adhesion-defects were generated and analyzed to determine the mutations responsible. In brief, 5000 M1 plants were mutagenized with EMS, and then self-crossed. M2 seeds were collected in pools and screened for adhesion defects using Ruthenium Red (RR), which binds de-eseterified pectin, but can only do so in hypocotyls when plants present decreased cellular adhesion (Kohorn et al 2021a, 2021b). The Kohorn lab identified numerous mutants, and one staining mutant line was identified in pool 242, exhibiting stunted hypocotyl and root growth alongside RR staining. The 242 line M2 exhibiting defective adhesion was self-crossed. The M3 offspring were then backcrossed to wild type plants to generate a heterozygous F1 generation, which did not stain, indicating that the causal mutation for RR staining was recessive. The F1 was self-crossed to segregate out background mutations among F2 offspring, which were stained with RR. Genomes of F2 offspring exhibiting RR staining were pooled and sequenced, as these individuals were presumed to be homozygous for the recessive causal mutation of staining.

Among the 13 mutations occurring at 100% frequency, one occurred in intergenic DNA and four in transposable elements (Fig. 2a, entries 2, 3, 6, 7, and 8). These mutations were assigned low priority for further investigation, as their loci were unlikely to be involved in adhesion pathways. Five additional mutations, those occurring in loci encoding a hypothetical protein, an amino acid transporter, HULK2, myosin4, and a mitochondrial protein, were positioned outside the ends of the coding regions of their respective loci (Fig. 2a, entries 1, 4, 5, 12, and 13). These were assigned low priority, as they were less likely to impact adhesion than mutations expected to produce translational changes. Of the three mutations remaining, one

occurred in the coding region of a gene encoding a lysine-rich repeat family protein, but was assigned low priority because it was predicted not to change the amino acid corresponding to its codon upon translation (Fig. 2a, entry 9).

The remaining two mutations were assigned high priority due to their likelihood of impacting gene expression (Fig 2a, red entries). One occurred in the single-exon coding region of At4g32390, which encodes a 350 amino acid sugar transporter (Fig. 2b). The mutation changed the 230th base in the coding region, a cytosine, to a thymine, generating a missense mutation substituting proline 77 in the wild type gene for leucine (Fig. 2b, navy text highlighted yellow). The mutation was assigned a high priority based on this amino acid sequence change. The other occurred at the 5' splice junction of exon 11 of *CesA1,* a primary cell wall cellulose synthase catalytic subunit (Fig. 2c). The mutation replaces the wild type thymine with a guanine. A change at a splice junction was expected to block splicing of the mRNA, so the mutation was assigned high priority. My thesis begins with the characterization of these two mutants.

(a)

Chromosome	Position	Reference	Mutation	Frequency	Depth	Gene Name	Gene ID	Protein Change		
1	4582287	G	A,<*>	1	13	AT1G13360	AT1G13360			hyp
1	14609269	C	G,T,<*>	1	28	AT1G39270	AT1G39270			TE
1	16601794	G	A,<*>	1	29	AT1G43835	AT1G43835			TE
2	16875951	C	T,<*>	1	16	AT2G40420	AT2G40420			aa transp
2	19697738	C	T,A,<*>	1	22	AT2G48160	AT2G48160			HULK2
4	1732875	G	A,<*>	1	10	AT4G03795-AT4G03800	AT4G03795-AT4G03800			
4	1740885	G	A,<*>	1	11	AT4G03800	AT4G03800			TE
4	9914031	C	A,T,<*>	1	39	AT4G17820	AT4G17820			TE
4	15181170	C	T,<*>	1	29	AT4G31250	AT4G31250	p.Lys194Lys		LRR
4	15636779	C	T,<*>	1	29	AT4G32390	AT4G32390	p.Pro77Leu		sugar transporter
4	15642663	C	T,<*>	1	46	CESA1	AT4G32410			splice junct
4	16328003	C	T,<*>	1	34	AT4G34080	AT4G34080			myosin4
Mt	91879	G	A,<*>	1	15	ORF145A	ATMG00300			

(b)

AT4G32390 242 sugar transporter

cctaaacatatatagttatatgcaattaatgtgaggcgagactaggaaacttaacatgaatggccaccaaatgtttgaacccaaaacaaaaactatatg
aattattaaggaaaaaaagataagtttcactcttttaacaaagtaatgttgacttataacaaccattgactactaataagattaaaagatgcatatttat
agttataaatagttaatgtaaacaagtaatttaattcatattgaatttaatattcacaaactgcaccaacctatcaaaattagtcaataaaaagaggtaa
gtgattaattaaacagtaaataagttagtgggcctatagataagcccattagtaaattggaaagaaaaaaacacctttaggccatagcacagtcacgcca
accctctcgctcgctacattagacagactctctcacaccaaaagtctctaaaaacacaacacacaaactgcgcattttatcctgcatccctcagacgacg
ctatcctgcgcaccaccgtcctcctccgttctcctcctcctccgagacaATGGGAAAAGGCGGTGCACTTAGCGATGGAGTCATCAAGAAGATCCTCCTC
TCCTACACCTACGTCGCGATCTGGATCTTCCTGAGCTTCACCGTCATCGTCTACAACAAATACATCCTCGACAAGAAGATGSALK<108775.56TACAA
TTGGCCTTTTCCGATCACACTCACCATGATCCACATGGCTTTTTGCTCTTCCCTCGCCGTCATCCTCATCAAAGTCTTCAAAATCGTCGAGCCTGTTTCA
ATGSALK089917C>TCTCGAGATACTTACATCAGATCTGTAGTCCCGATCGGTGCTCTGTACTCGCTTTCTCTCTGGCTCTCCAATTCCGCTTACATTT
ACCTCTCCGTCTCCTTCATTCAGATGCTCAAAGCTCTAATGCCTGTCGCTGTTTACTCAATCGGAGTCCTTCTTAAGAAAGAATCGTTCAAATCGGAGAC
GATGACTAATATGCTCTCGATCTCTTTCGGTGTTGCGATTGCTGCTTATGGTGAGGCTAAGTTCGATACTTGGGGAGTTATGCTTCAGCTTGGTGCTGTA
GCTTTCGAAGCAACGAGGTTGGTTTTGATTCAGATCTTGCTCACTTCTAAAGGAATCAATCTTAATCCAATCACTTCATTGTACTACGTTGCTCCTTGTT
GTTTGGTGTTCCTCTTCTTCCCTTGGATCTTCGTCGAGCTTCCGATTCTTAGGGAAACTTCGAGTTTCCACTTTGATTTCGTGATTTTTGGGACTAATTC
CGTATGTGCATTTGCTTTGAACCTTGCTGTGTTCCTCCTCGTTGGAAAGACCTCGGCTTTAACAATGAATGTTGCTGGTGTGGTTAAGGATTGGCTATTG
ATTGCCTTCTCTTGGTCTGTGATTAAAGATACGGTGACTCCGCTTAATCTCTTTGGTTACGGGCTTGCGTTCTTGGGTGTTGCGTATTACAATCACTGCA
AGTTACAGGCGTTGAAGGCTAAGGATGCTCAGAAGAAGGTTCAGCAAGGTGATGAAGAAGAAGCTGGGAAGCTTTTGGAAGAGAGGGAAAGTGAAGCTGC
TGCGAAACGGAATGAAACAGAAGACTGAttgagttgatgatcataaggaaaggtttgtgaatttgatgaatgtgtggaattcagaggaataagagttgaa
gtgttaggatgattttggtagctttggaggaaaattttcaacaggattttgcgcatcatctttggttcacttctttgcttaggtatgatcgtctttctta
ttgtcaatctctctggttttgagttttagttgctatgttacttttaagttatggctgattatatttacatagtggatttgatggtacaaggattttagaa
gttttaatgtctttgtgatgatttacaatgtaccactcggatcttgtgttctatggagttttctttgtttcttatgaatctattttggtttacttttata
atgccattgagatcctgtttggttctaagttattatcaagattcaagataaagatgttaaaagcat

(c)

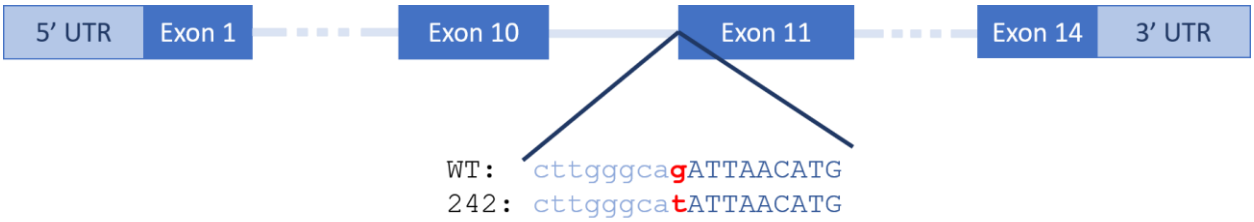

Figure 2. (a) List of mutations occurring at 100% frequency among RR-staining mutant line 242 F2 offspring. High-priority entries are in red text. The *A. thaliana* col. Version 10 genome was used to determine positions. "Mutation" indicates that the wild type allele changed to the indicated base. (b) At4g32390 sequence encoding a Golgi sugar transporter. The coding region is yellow, with start and stop codons highlighted blue. Yellow highlight shows the mutant allele. T-DNA insertion sites are marked with green and orange SALK labels. Primer sites are underlined. (c) Schematic representation of the *CesA1* mutation at the intron/exon 11 junction found in line 242 F2 seedlings.

At4g32390 has been implicated in transport of L-arabinose, a key component of RG-I (Rautengarten et al. 2017). Neither morphological divergence from wild type nor RR staining has been reported in At4g32390 knock-out plants, but overexpression of the gene was associated with a 30% increase of L-arabinose in cell walls and epitopes corresponding to increases in RG-I, RG-I-associated arabinogalactans, and arabinogalactan proteins (Rautengarten et al. 2017). Strong *CesA1* mutants have demonstrated development defects as seen in line 242 but have not been reported to stain with RR. One possible explanation for line 242's combination of phenotypes was the *CesA1* mutation produced the stunted hypocotyl and root phenotype, while the At4g32390 mutation caused staining. Another was that the *CesA1* mutations was responsible for both the stunted and staining phenotypes.

Mutations to At4g32390 are not implicated in Ruthenium Red staining

In order to investigate the role of the sugar transporter in RR staining, two different SALK lines with T-DNA insertions targeting the sugar transporter coding region were obtained from the Arabidopsis stocks center (ABRC) (Fig 2b, orange and green text). Unlike the proline-leucine substitution allele present in 242 plants, which could produce a strong change in function of the protein or none at all, the T-DNA insertions would be expected to knock out At4g32390. SALK_108775 targeted the position between the 132nd and 133rd bases of the coding region for T-DNA insertion (Fig 2b, orange). SALK_089917C targeted the position between the 240th and 241st bases of the coding region (Fig. 2b, green). If the gene was transcribed and translated with the insertions at these positions, only the N-terminal 80 and 96 amino acids of 350 would likely be properly translated before a stop codon arose in the insert sequence. With less than one third

of the protein correctly translated, it is unlikely to fulfill its function. A homozygote for two null alleles could be used to assess whether lack of protein function was responsible for staining.

To produce seedlings homozygous for a T-DNA insert allele, seeds from each of the two SALK lines were grown in soil, DNA was extracted from leaves, and the plants were genotyped via PCR. Different sets of primers were used to detect each of the wild type and T-DNA insertion alleles. To detect the insert in SALK_108775 plants, a forward primer corresponding to wild type DNA and a reverse primer corresponding to the T-DNA insert were used (Fig. 3a, orange arrows). If and only if the insertion was present could the reverse primer anneal, amplification proceed, and a 576-bp product form. To detect the insert in SALK_0089917C plants, a forward primer corresponding to the T-DNA insert and a reverse primer corresponding to wild type DNA were used (Fig. 3a, green arrows). If and only if the insertion was present could the forward primer anneal and a 625-bp product form. Primers corresponding to wild type DNA that flanked both insertion sites were used to detect the wild type allele (Fig 3a, blue arrows). If no insertion was present, a 695 bp product was expected. If either insertion was present, too much DNA would lie between the primers to complete PCR elongation under the experimental conditions, so no product would form.

Gel electrophoresis of PCR to detect T-DNA inserts in each SALK line produced no bands for the 6 SALK_108775 plants tested, suggesting that the reverse primer had failed to anneal due to a lack of T-DNA. Of the 6 plants tested, a band of the expected size of 625 bp was amplified for only plant #5 from the SALK_089917C line, indicating that it alone possessed the inserted T-DNA (Fig. 3b).

PCR for the wild-type allele of At4g32390 produced the expected 695 bp band for a WT control and SALK plants tested except for plant #5 from the SALK_089917C line, indicating

that the plant was homozygous for the insertion, as all alelles must have had T-DNA to interfere with elongation (Fig. 3c). Sequencing of the insert band confirmed that the T-DNA had been inserted after base 240 of the exon.

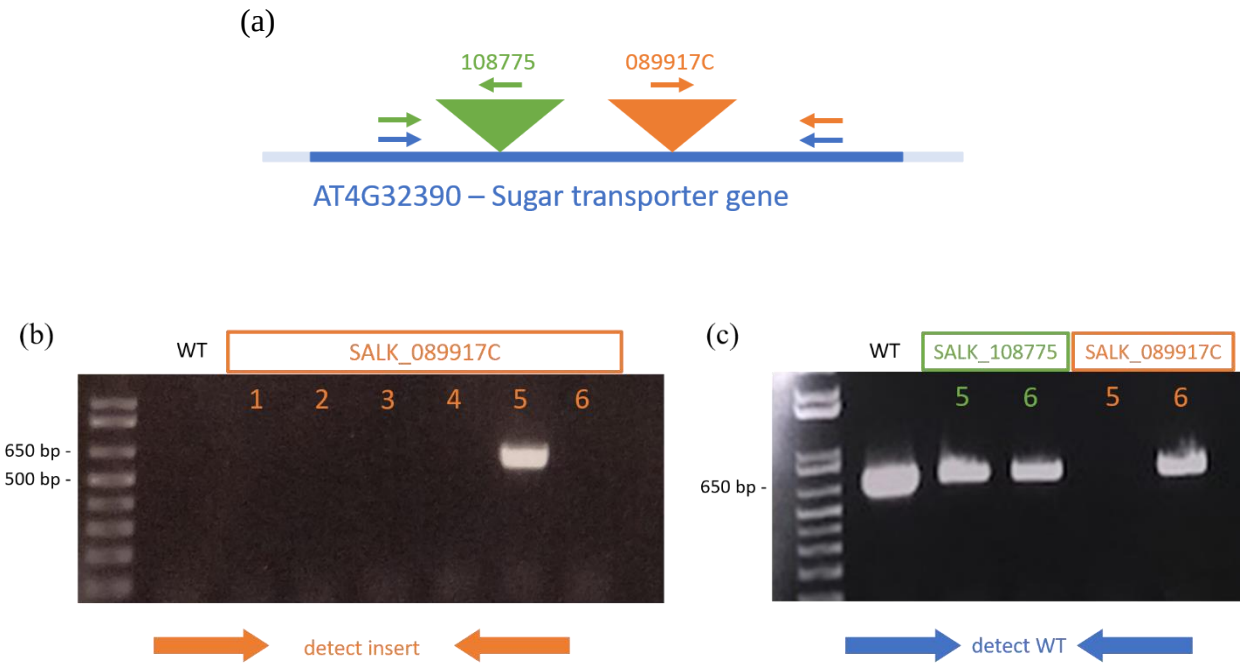

Figure 3. Sugar transporter mutant genotyping. (a) Representative schematic for PCR genotyping. The SALK_108775 T-DNA insert is indicated by the green triangle. The SALK_089917C T-DNA insert is indicated by the orange triangle. Green arrows represent primers for SALK_108775 T-DNA detection. Orange arrows represent primers for SALK_089917C T-DNA detection. Blue arrows represent primers for wild-type allele detection. (b) PCR for a T-DNA insert in At4g23290 in a Columbia control (WT) and six SALK_089917C plants. (c) PCR for the wild type allele At4g23290 in a Columbia control (WT), two SALK_108775 plants, and two SALK_089917C plants.

To assess the role of the sugar transporter in mutant line 242 RR staining, the SALK_089917C plant homozygous for the insertion was self-crossed, and the F1 offspring were dark grown in liquid media and screened for adhesion defects using RR. The seedling hypocotyls did not take up the dye, and their hypocotyl cells did not exhibit adhesion defects (Fig. 4). Given that these seedlings were homozygous for a null allele of At4g32390, these results indicate that

loss of function of the sugar transporter encoded by the gene are likely not solely responsible for the RR staining in line 242 seedlings, nor is this sugar transporter essential for proper cell adhesion.

CesA1 is essential for proper cell adhesion

To assess the potential role of CesA1 in mutant line 242 staining, plants homozygous for *rsw1-1,* a temperature sensitive and partially penetrant mutation of *CesA1,* were grown in soil and self-crossed, and their offspring were collected, dark grown in liquid media, and stained with RR. All offspring were either moderately stunted or severely stunted (Fig. 4, bottom row), as the allele has been reported to be partially penetrant and partially temperature sensitive, leading to a degree of phenotypes within a population grown at 25°C (Arioli et al. 1998). While stunted but less effected *rsw1-1*$^{-/-}$ hypocotyls did not stain, the severely stunted *rsw1-1*$^{-/-}$ seedlings stained throughout, mirroring the staining pattern of mutant line 242 (Fig. 4, top center, bottom row). The similarities in these staining patterns indicate that the CesA1 mutation is responsible for line 242 staining.

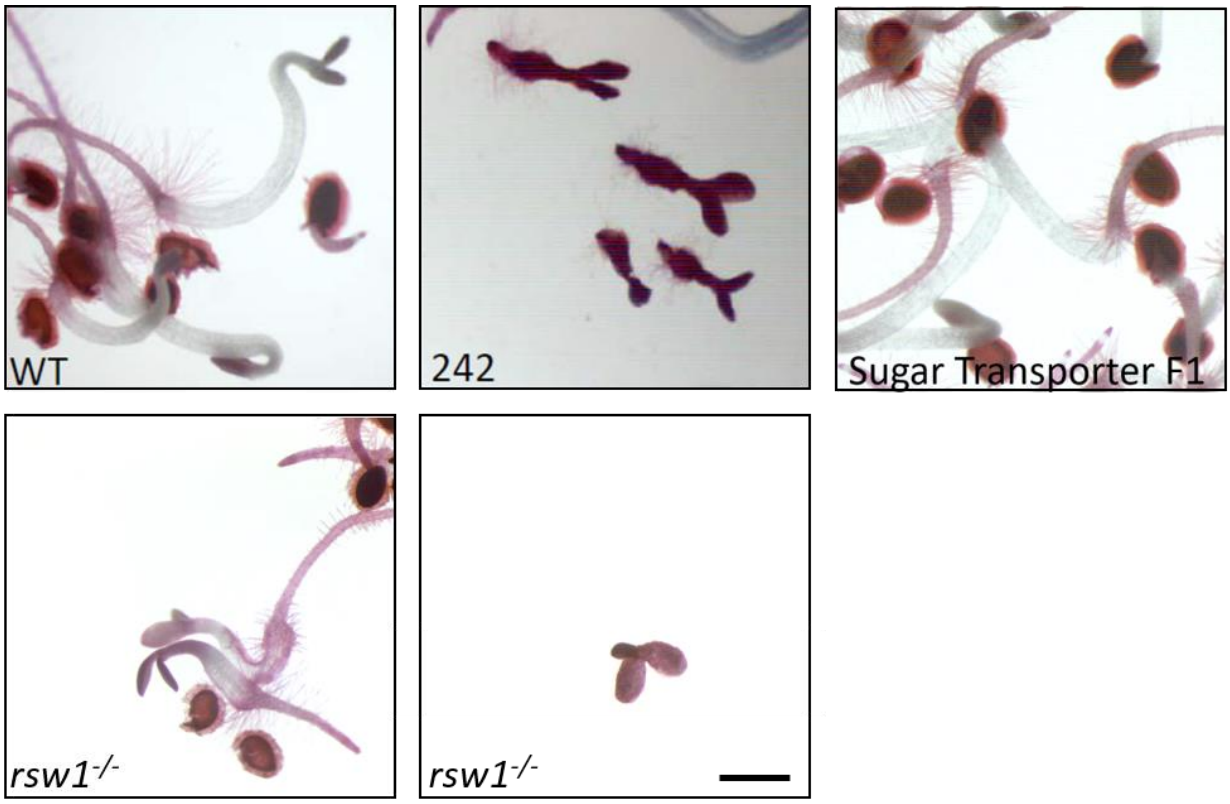

Figure 4. Seedlings homozygous for *CesA1* mutations stain throughout with RR. RR assays of dark-grown four-day-old wild type seedlings, 242 mutant line seedlings, seedlings homozygous for a T-DNA insert into At4g23290, and *rsw1-1*$^{-/-}$seedlings. Bottom left and right panel of show the two types of phenotypes seen in the temperature sensitive and partially pentrant *rsw1-1*$^{-/-}$ mutant population. Scale bar is 1 mm.

The stunted growth in the *rsw1-1*$^{-/-}$ seedlings suggests that the *CesA1* mutation is responsible for stunted growth in line 242. It is unknown whether the mutant *CesA1* transcript in line 242 is translated. If it is, the decreased severity of this phenotype in line 242 seedlings relative to highly effected *rsw1-1*$^{-/-}$ seedlings may be a reflection of the relative strengths of the alleles. Line 242's point substitution in the splice junction at the 5' end of *CesA1* Exon 11, and is thus expected to impact mRNA splicing. Proper transcription and translation of the first ten exons may preserve some degree of the CesA1's structure and function while still causing enough functional loss to disrupt ECM architecture and cellular adhesion, allowing RR to enter

and stain. These findings indicate that sufficient levels of CesA1 activity are necessary for typical cellular adhesion.

ELMO2 and ELMO3 are Golgi proteins

The Kohorn lab previously identified a mutation in the ELMO1 Golgi protein that leads to an adhesion-defect. ELMO1 has four additional highly similar homologs ELMO2-5 encoded by the *A. thaliana* genome. *ELMO2* (At1g05070) and *ELMO3* (At4g04360) are predicted to also encode Golgi-localized proteins, and while elmo2$^{-/-}$ and elmo3$^{-/-}$ single mutants appear similar to WT, *elmo1-1*$^{-/-}$*elmo2*$^{-/-}$ double mutant seedlings exhibit severe cell adhesion defects, stronger than *elmo1-1*$^{-/-}$ single mutants. These results suggest that the proteins encoded by *ELMO1* and *ELMO2*, and perhaps the other *ELMO* family members, might play partially redundant roles in cell adhesion pathways. To further characterize ELMO2 and ELMO3 each gene was cloned with a carboxyl-terminal GFP marker, and the cloned plasmids were used to localize the fusion protein in transiently transformed protoplasts expressing RFP markers for Golgi and ER compartments (Fig. 5a).

The *ELMO2* and *ELMO3* coding regions from genomic DNA extracted from Col-0 leaves were PCR amplified using a forward primer that appended an NcoI restriction site upstream of the start codon and a reverse primer that replaced the stop codon of *ELMO2* with a SpeI restriction site and the stop codon of *ELMO3* with a BglII restriction site (Fig. 5b). Each PCR reaction using genomic DNA as template produced the expected sized bands: 1360 bp for *ELMO2* and 726 bp for *ELMO3* (Fig. 5c, note ELMO2 contains an intron). The insert bands were extracted and cloned into pSC-A, and StrataClone competent *E. coli* (Agilent) were transformed with the vector. The cloned fusion gene was isolated via alkaline lysis and digested

using the appropriate restriction enzymes for each clone to generate ELMO-GFP inserts with sticky ends. Gel electrophoresis of the digest produced bands at the same positions as the PCR, indicating the presence of the insert, as well as bands at approximately 3.7 kb and 600 bp, reflecting non-insert vector DNA cut into two fragments at pSC-A's NcoI site (Fig. 5d). The ELMO-GFP inserts were extracted from the gel and cloned into pCambia1302 to generate the ELMO-GFP constructs that were driven by a constitutive viral promoter. Presence of the insert was detected by gel electrophoresis of restriction enzyme digested plasmid preparations from transformed DH5-α cultures, as indicated by bands at the same positions as from the PCR (Fig. 5e).

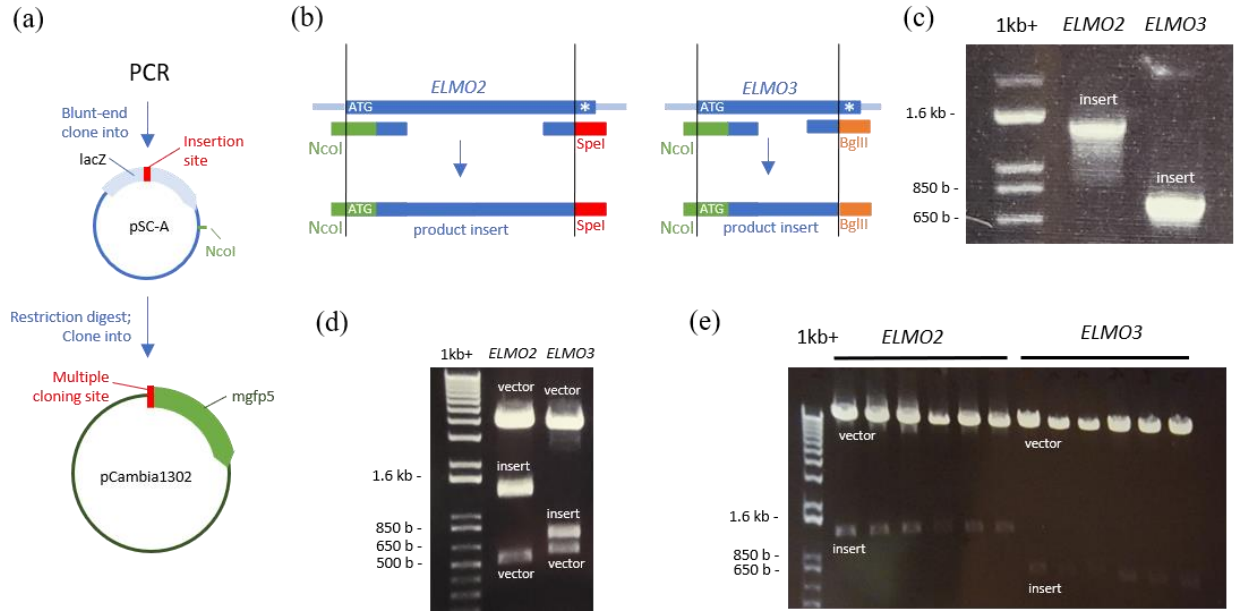

Figure 5. Cloning to generate vectors expressing ELMO-GFP fusions. (a) Schematic representation of cloning approach. (b) Schematic representation of *ELMO2* and *ELMO3* PCR. (c) PCR amplification of *ELMO2* and *ELMO3* coding regions. (d) Digests of pSC-AELMO2 preparation by NcoI and SpeI and pSC-AELMO3 preparation by NcoI and BglII to confirm the presence of and isolate cloned inserts. (e) Digests of pCambia1302ELMO2 preparations by NcoI and SpeI and pCambia1302ELMO3 preparations by NcoI and BglII to detect cloned insert presence.

To determine the subcellular localization of ELMO2- and ELMO3-GFP fusions, protoplasts from plants expressing mCherry fusion proteins – ATMEMB12 in the Golgi and AT-NLM1 in the endoplasmic reticulum (ER) – were transformed using either pCambia1302ELMO2-GFP or pCambia1302ELMO3-GFP to express ELMO-GFP fusions under the control of the viral 35S promoter. In Golgi marker protoplasts, confocal microscopy revealed overlap between strong GFP and RFP signals, while in ER marker protoplasts, there was no overlap between strong GFP and RFP signals (Fig. 6). 35S:ELMO2::GFP and 35S:ELMO2::GFP localize to the Golgi and not the ER, indicating that ELMO2 and ELMO3, like ELMO1, are Golgi proteins. In Golgi RFP protoplasts, there were points of strong GFP but not RFP signal, indicating that the ELMO-GFP fusions partially localized to non-Golgi compartments (Fig. 6, rows 1 and 3). This mismatched signal is likely the product of overexpression of the GFP fusions, which might have overloaded cellular transport systems and led to displacement of excess GFP-tagged protein to other compartments. Additionally, mCherry detection presented high levels of background signal in all cases. This background was likely produced by chlorophyll degraded in the transformation or microscopy conditions, which would be expected to exhibit altered emission spectra.

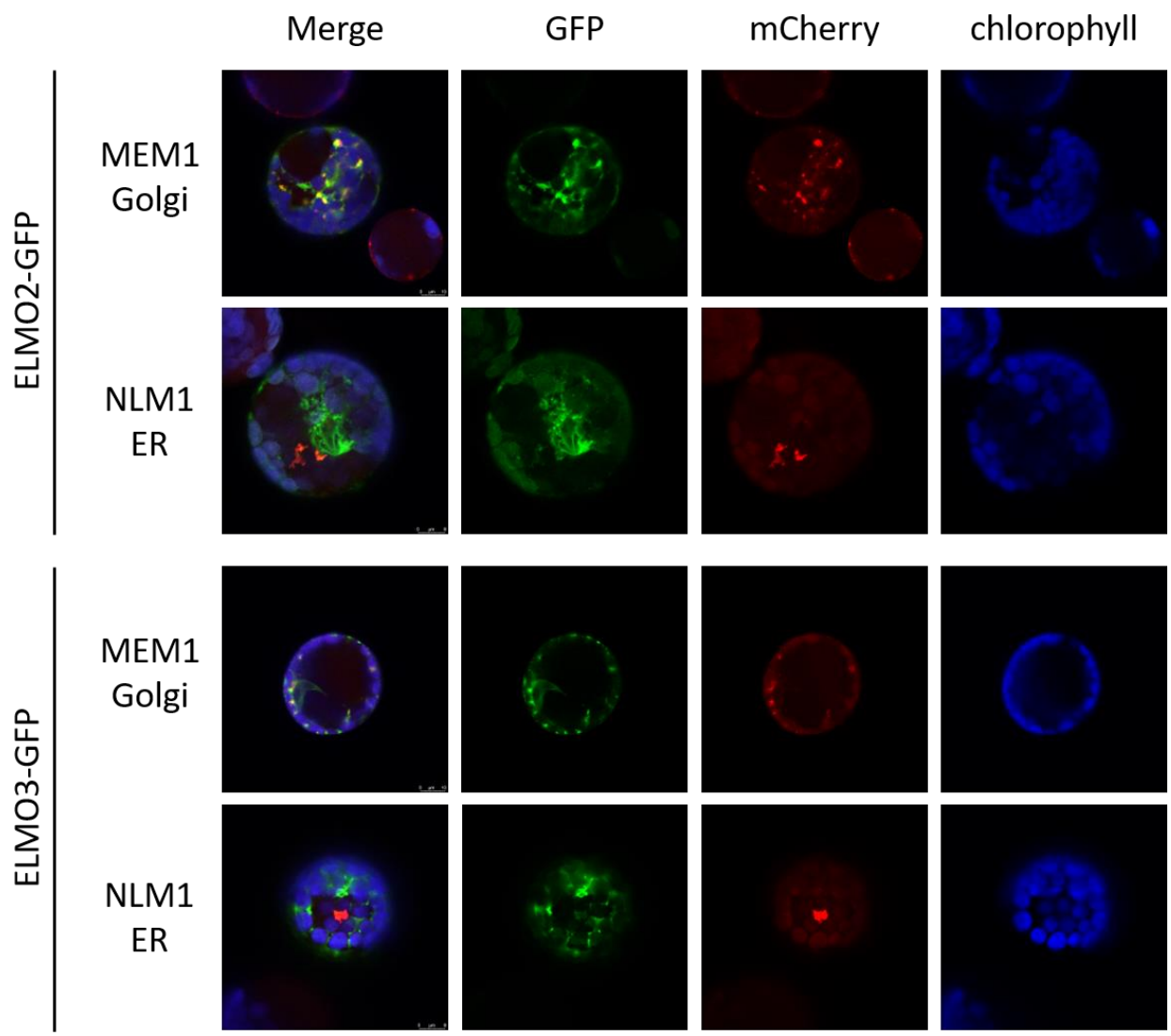

Figure 6. 35S:ELMO2::GFP and 35S:ELMO2::GFP colocalize with Golgi and not ER markers. Either 35S:ELMO2::GFP or 35S:ELMO2::GFP was expressed in Wave line protoplasts expressing either mCherry tagged MEM1 in the Golgi or NLM1 in the ER. Protoplasts were visualized using confocal microscopy. GFP emission is green, mCherry emission is red, and chlorophyll emission is blue. Bar is 10 µm.

Discussion

Cell adhesion mediated by the ECM plays a key role in plant morphology, growth, and development. While some highly structured tissues require cells to stay in place relative to their neighbors, other fundamental plant processes, such as abscission and dehiscence, necessitate the

controlled separation cells. Thus, plants have developed a vast regulatory system for managing cellular adhesion. Early understandings of these pathways held that the level of adhesion between cells was primarily governed by HG pectin levels in the middle lamella. However, more recent findings complicate adhesion models, indicating that these processes are governed by a largely uncharacterized signaling pathway with connections to pectin synthesis, methylesterification, and degradation, as well as activity of Golgi proteins ELMO1, ESMD1 and FRB1 (Neumetzler et al. 2012; Verger et al. 2016). In order to deepen our understanding of adhesion pathways, Ruthenium Red (RR) staining was used to identify new adhesion mutants among EMS mutagenized *A. thaliana*. This thesis details work to identify the causal mutation for the adhesion phenotype of RR staining in one of these mutant lines, 242, as well as localization studies for homologs of ELMO1, a putative Golgi scaffold protein necessary for typical plant cell adhesion identified in another line from the mutant screen (Kohorn et al. 2021b).

CesA1 and adhesion

Two mutations in line 242 RR staining plants were identified as high priority for investigation: a missense mutation in At4g32390, predicted to encode a Golgi sugar transporter, and a substitution in a splice junction on the 5' border of Exon 11 of *CesA1*, which encodes a catalytic subunit of cellulose synthase implicated associated with the primary cell wall. In order to assess the potential contribution of each mutation to the staining phenotype, single mutant seedlings homozygous for mutations in one of these genes or the other were generated and assayed with RR. Seedlings homozygous for the sugar transporter null mutation did not stain, while *rsw1-1*$^{-/-}$ seedlings, homozygous for a temperature-sensitive *CesA1* mutant allele, did.

These results implicate line 242's *CesA1* mutation as solely responsible for RR staining and the atypical cellular adhesion it reflects.

There appear to be no previous reports of plants with cellulose synthase mutations exhibiting adhesion defects or RR staining, and cellulose is not typically considered a key player in adhesion processes. However, the mutations in *QUA2,* known to produce adhesion defects, were recently shown to disrupt cellulose synthesis, decreasing cellulose content, slowing cellulose synthase particles, disrupting cellulose organization, and increasing cellulose mobility (Du et al. 2020). Microtubules, along which cellulose synthase complexes travel during cellulose deposition, exhibited aberrant organization and abnormal propensity for depolymerization, suggesting that disruption of the pectin network altered microtubule and cellulose patterning and decreased the rate of cellulose synthesis and deposition in the ECM (Du et al. 2020). Mutations in the microtubule organizing, membrane protein SABRE can also suppress pectin dependent adhesion defects, further supporting a relationship between the cytoskeleton and pectin in the cell wall (Kohorn et al 2021a). This model reflects an interplay between HG pectin and cellulose networks, and decreased levels and increased mobility of both pectin and cellulose might alter the interactions between ECM pectin, cellulose, and microtubule networks, possibly contributing to a lack of adhesion between cells. Interruptions to cellulose synthesis via *CesA1* mutations might decrease cellulose content, altering the interactions between cellulose in the primary wall and other ECM networks, disrupting the organization of those networks responsible for adhesion, and preventing structures from anchoring to one another.

ELMO family member localization

ELMO1, a Golgi protein, was previously identified through a mutant screen as necessary for proper adhesion (Kohorn et al. 2021b). Sequence analysis revealed four additional *ELMO1* homologs in the *A. thaliana* genome. Subsequent studies of these homologs revealed that dark grown seedlings of *elmo2*$^{-/-}$ and *elmo3*$^{-/-}$ single mutants appeared like wild type and did not stain with RR, but *elmo1*$^{-/-}$*elmo2*$^{-/-}$ double mutants exhibited stronger adhesion defects than *elmo1*$^{-/-}$ single mutants, indicating that ELMO2, and in turn other homologs, might play a partially redundant role to ELMO1 in adhesion pathways. To contribute to the characterization of the ELMO family members and their potential roles in plant cell adhesion, subcellular localization studies were performed with ELMO2-GFP and ELMO3-GFP fusions in protoplasts expressing mCherry markers for either the Golgi or ER. Both 35S:ELMO2::GFP and 35S:ELMO3::GFP colocalized with Golgi but not ER markers, indicating that ELMO2 and ELMO3, like ELMO1, are Golgi proteins. The imaging process produced high levels of background emission from chlorophyll, which could be reduced via stable transformation of plants with *Agrobacterium tumefaciens*, allowing for clearer imaging of colocalization in offspring cells of tissues lacking chloroplasts (Clough and Bent, 1998). This stable transformation will also reduce the extent of overexpression of the *ELMO-GFP* constructs seen in the transient gene expression in protoplasts, increasing the precision of localization.

The Golgi localization of ELMO2 and ELMO3 is consistent with predictions that they might serve partially redundant roles to ELMO1 in adhesion pathways. Structurally, ELMO1 is predicted to possess a signal sequence, a membrane anchor, a Golgi lumenal domain, and a coiled-coil structure, but it is not predicted to exhibit similar structure to any known enzyme classes, suggesting that it and its homologs might act as accessory or scaffold proteins, perhaps

in mannose-related quality control mechanisms for cell wall proteins, an adhesion related signal transduction pathway, or synthesis of ECM carbohydrates (Kohorn et al. 2021b). Scaffold proteins facilitate signaling and catalytic processes by recruiting and holding proteins in a complex (Lim et al. 2019). Protein complex formation has been identified in plant carbohydrate synthesis pathways, including starch synthesis in wheat (Tetlow et al. 2008), and scaffold proteins are implicated in a wide range of processes in Arabidopsis, including the Cullins in ubiquitination (Gingerich et al. 2005), the BTB and TAZ domain proteins in gametophyte development (Robert et al. 2007), RACK1A in stress and photosynthetic pathways (Kundu et al. 2013), and an amylose-binding protein in chloroplast starch metabolism (Lohmeier-Vogel et al. 2008). Determining which proteins ELMO family members interact with will be a key element in elucidating their role in adhesion pathways. Immunoprecipitation of ELMO-GFP fusions and any associated proteins from plant cell extracts might reveal these interactions.

While *elmo1*$^{-/-}$ plants do not reflect decreased pectin levels, plants with mutations in another of the homologs, ELMO4, do have reduced pectin levels, and BiFc shows interaction between ELMO4 and QUA1, suggesting that ELMO4 is involved in pectin synthesis (Pearsson unpublished). The *elmo4*$^{-/-}$ plants exhibit stronger hypocotyl cell peeling and RR staining than *elmo1*$^{-/-}$ plants (Kohorn et al. 2021b). It is possible that the other ELMO family proteins might also be involved in pectin synthesis pathways, but the effects of single mutations to each other family member alone might be too slight to be detectable. Analysis of pectin and other polysaccharide content in ELMO family double mutants might reveal clearer connections to adhesion pathways.

In summary, this thesis identifies CesA1 as necessary for cellular adhesion in Arabidopsis, suggesting that adhesion networks may be dependent on structural cellulose to

some extent. This work has also identified ELMO2 and ELMO3 as Golgi proteins, the same location as ELMO1, and together they likely form redundant components of a scaffold for pectin synthesis.

REFERENCES

Alonso J, Canet W, Rodriguez T (1997) Thermal and calcium pretreatment affects texture, pectinesterase and pectic substances of frozen sweet cherries. *Journal of Food Science* 62 (3):511-515

Arioli T, Peng L, Betzner AS, Burn J, Wittke W, Herth W, Camilleri C, Höfte H, Plazinski J, Birch RJS (1998) Molecular analysis of cellulose biosynthesis in Arabidopsis. *Science* 279 (5351):717-720

Atmodjo MA, Hao Z, Mohnen D (2013) Evolving views of pectin biosynthesis. *Annual review of plant biology* 64:747-779

Baskin TI (2005) ANISOTROPIC EXPANSION OF THE PLANT CELL WALL. *Annual Review of Cell and Developmental Biology* 21 (1):203-222. doi:10.1146/annurev.cellbio.20.082503.103053

Beeckman T, Przemeck GK, Stamatiou G, Lau R, Terryn N, De Rycke R, Inzé D, Berleth T (2002) Genetic complexity of cellulose synthase A gene function in Arabidopsis embryogenesis. *Plant Physiology* 130 (4):1883-1893

Bouton S, Leboeuf E, Mouille G, Leydecker M-T, Talbotec J, Granier F, Lahaye M, Höfte H, Truong H-N (2002) QUASIMODO1 Encodes a Putative Membrane-Bound Glycosyltransferase Required for Normal Pectin Synthesis and Cell Adhesion in Arabidopsis. *The Plant Cell* 14 (10):2577-2590. doi:10.1105/tpc.004259

Braccini I, Pérez S (2001) Molecular basis of Ca2+-induced gelation in alginates and pectins: the egg-box model revisited. *Biomacromolecules* 2 (4):1089-1096

Brown Jr RM (1996) The biosynthesis of cellulose. *JJoMS* 33 (10):1345-1373

Cabrillac D, Cock JM, Dumas C, Gaude T (2001) The S-locus receptor kinase is inhibited by thioredoxins and activated by pollen coat proteins. *Nature* 410 (6825):220-223

Caffall KH, Mohnen D (2009) The structure, function, and biosynthesis of plant cell wall pectic polysaccharides. *Carbohydrate Research* 344 (14):1879-1900. doi:https://doi.org/10.1016/j.carres.2009.05.021

Claugh SJ, Bent AF (1998) Floral dip: a simplified method for Agrobacterium-mediated transformation of Arabidopsis thaliana. Plant Journal 16, 735-743.

Cosgrove DJ (1997) Assembly and enlargement of the primary cell wall in plants. *Annual Review of Cell and Developmental Biology* 13 (1):171-201. doi:10.1146/annurev.cellbio.13.1.171

Daher FB, Braybrook SA (2015) How to let go: pectin and plant cell adhesion. *Frontiers in Plant Science* 6 (523). doi:10.3389/fpls.2015.00523

Decreux A, Messiaen J (2005) Wall-associated Kinase WAK1 Interacts with Cell Wall Pectins in a Calcium-induced Conformation. *Plant and Cell Physiology* 46 (2):268-278. doi:10.1093/pcp/pci026

Decreux A, Thomas A, Spies B, Brasseur R, Van Cutsem P, Messiaen J (2006) In vitro characterization of the homogalacturonan-binding domain of the wall-associated kinase WAK1 using site-directed mutagenesis. *Phytochemistry* 67 (11):1068-1079

Denès J-M, Baron A, Renard CM, Péan C, Drilleau J-F (2000) Different action patterns for apple pectin methylesterase at pH 7.0 and 4.5. *Carbohydrate Research* 327 (4):385-393

Desprez T, Vernhettes S, Fagard M, Refrégier G, Desnos T, Aletti E, Py N, Pelletier S, Höfte H (2002) Resistance against Herbicide Isoxaben and Cellulose Deficiency Caused by Distinct Mutations in Same Cellulose Synthase Isoform CESA6. *Plant Physiology* 128 (2):482-490. doi:10.1104/pp.010822

Dick-Pérez M, Zhang Y, Hayes J, Salazar A, Zabotina OA, Hong M (2011) Structure and Interactions of Plant Cell-Wall Polysaccharides by Two- and Three-Dimensional Magic-Angle-Spinning Solid-State NMR. *Biochemistry* 50 (6):989-1000. doi:10.1021/bi101795q

Downie B, Dirk LM, Hadfield KA, Wilkins TA, Bennett AB, Bradford KJ (1998) A gel diffusion assay for quantification of pectin methylesterase activity. *Analytical biochemistry* 264 (2):149-157

Drakakaki G (2015) Polysaccharide deposition during cytokinesis: Challenges and future perspectives. *Plant Science* 236:177-184. doi:https://doi.org/10.1016/j.plantsci.2015.03.018

Du J, Kirui A, Huang S, Wang L, Barnes WJ, Kiemle SN, Zheng Y, Rui Y, Ruan M, Qi S, Kim SH, Wang T, Cosgrove DJ, Anderson CT, Xiao C (2020) Mutations in the Pectin Methyltransferase QUASIMODO2 Influence Cellulose Biosynthesis and Wall Integrity in Arabidopsis. *The Plant Cell* 32 (11):3576-3597. doi:10.1105/tpc.20.00252

Dwyer KG, Kandasamy MK, Mahosky DI, Acciai J, Kudish BI, Miller JE, Nasrallah ME, Nasrallah JB (1994) A superfamily of S locus-related sequences in Arabidopsis: diverse structures and expression patterns. *The Plant Cell* 6 (12):1829-1843

Endler A, Persson S (2011) Cellulose Synthases and Synthesis in Arabidopsis. *Molecular Plant* 4 (2):199-211. doi:https://doi.org/10.1093/mp/ssq079

Fagard M, Desnos T, Desprez T, Goubet F, Refregier G, Mouille G, McCann M, Rayon C, Vernhettes S, Höfte H (2000) PROCUSTE1 Encodes a Cellulose Synthase Required for Normal Cell Elongation Specifically in Roots and Dark-Grown Hypocotyls of Arabidopsis. *The Plant Cell* 12 (12):2409-2423. doi:10.1105/tpc.12.12.2409

Fleischer A, O'Neill MA, Ehwald R (1999) The pore size of non-graminaceous plant cell walls is rapidly decreased by borate ester cross-linking of the pectic polysaccharide rhamnogalacturonan II. *Plant Physiology* 121 (3):829-838

Francis KE, Lam SY, Copenhaver GP (2006) Separation of Arabidopsis pollen tetrads is regulated by QUARTET1, a pectin methylesterase gene. *Plant physiology* 142 (3):1004-1013

Geldner N, Dénervaud-Tendon V, Hyman DL, Mayer U, Stierhof YD, Chory J (2009) Rapid, combinatorial analysis of membrane compartments in intact plants with a multicolor marker set. Plant Journal 59 (1):169-178. doi: 10.1111/j.1365-313X.2009.03851.x.

Gillmor CS, Poindexter P, Lorieau J, Palcic MM, Somerville C (2002) α-Glucosidase I is required for cellulose biosynthesis and morphogenesis in Arabidopsis. *Journal of Cell Biology* 156 (6):1003-1013. doi:10.1083/jcb.200111093

Gingerich DJ, Gagne JM, Salter DW, Hellmann H, Estelle M, Ma L, Vierstra RD (2005) Cullins 3a and 3b Assemble with Members of the Broad Complex/Tramtrack/Bric-a-Brac (BTB)

Protein Family to Form Essential Ubiquitin-Protein Ligases (E3s) in Arabidopsis. *Journal of Biological Chemistry* 280 (19):18810-18821. doi:https://doi.org/10.1074/jbc.M413247200
Hansen SF, Harholt J, Oikawa A, Scheller HV (2012) Plant glycosyltransferases beyond CAZy: a perspective on DUF families. *Frontiers in plant science* 3:59
He Z-H, Cheeseman I, He D, Kohorn BD (1999) A cluster of five cell wall-associated receptor kinase genes, Wak1–5, are expressed in specific organs of Arabidopsis. *Plant molecular biology* 39 (6):1189-1196
Hill JL, Jr., Hammudi MB, Tien M (2014) The Arabidopsis cellulose synthase complex: a proposed hexamer of CESA trimers in an equimolar stoichiometry. *The Plant Cell* 26 (12):4834-4842. doi:10.1105/tpc.114.131193
Höfte H, Peaucelle A, Braybrook S (2012) Cell wall mechanics and growth control in plants: the role of pectins revisited. *Plant Physiology* 3 (121). doi:10.3389/fpls.2012.00121
Hong MJ, Kim DY, Lee TG, Jeon WB, Seo YW (2010) Functional characterization of pectin methylesterase inhibitor (PMEI) in wheat. *Genes genetic systems* 85 (2):97-106
Iwai H, Ishii T, Satoh S (2001) Absence of arabinan in the side chains of the pectic polysaccharides strongly associated with cell walls of Nicotiana plumbaginifolia non-organogenic callus with loosely attached constituent cells. *Planta* 213 (6):907-915
Iwai H, Masaoka N, Ishii T, Satoh S (2002) A pectin glucuronyltransferase gene is essential for intercellular attachment in the plant meristem. *PNAS* 99 (25):16319-16324
Jarvis MC, Briggs SPH, Knox JP (2003) Intercellular adhesion and cell separation in plants. *Plant, Cell, and Environment* 26 (7):977-989. doi:https://doi.org/10.1046/j.1365-3040.2003.01034.x
Ji D, Chen T, Zhang Z, Li B, Tian S (2020) Versatile Roles of the Receptor-Like Kinase Feronia in Plant Growth, Development and Host-Pathogen Interaction. *Int J Mol Sci* 21 (21):7881. doi: https://doi.org/10.3390/ijms21217881
Jolie RP, Duvetter T, Houben K, Vandevenne E, Van Loey AM, Declerck PJ, Hendrickx ME, Gils A (2010) Plant pectin methylesterase and its inhibitor from kiwi fruit: Interaction analysis by surface plasmon resonance. *Food chemistry* 121 (1):207-214
Kim K, Yi H, Zamil MS, Haque MA, Puri VM (2015) Multiscale stress-strain characterization of onion outer epidermal tissue in wet and dry states. *American Journal of Botany* 102 (1):12-20
Kim S-J, Brandizzi F (2014) The plant secretory pathway: an essential factory for building the plant cell wall. *Plant cell physiology* 55 (4):687-693
Kimura S, Laosinchai W, Itoh T, Cui X, Linder CR, Brown RM (1999) Immunogold labeling of rosette terminal cellulose-synthesizing complexes in the vascular plant Vigna angularis. *JTPC* 11 (11):2075-2085
Klemm D, Heublein B, Fink H-P, Bohn A (2005) Cellulose: Fascinating Biopolymer and Sustainable Raw Material. *Angewandte Chemie International Edition* 44 (22):3358-3393. doi:https://doi.org/10.1002/anie.200460587
Knox JP (1992) Cell adhesion, cell separation and plant morphogenesis. *The Plant Journal* 2 (2):137-141. doi:https://doi.org/10.1111/j.1365-313X.1992.00137.x
Kohorn BD (2016) Cell wall-associated kinases and pectin perception. *J Exp Bot.* 67:489-94
Kohorn BD (2015) The State of Cell Wall Pectin Monitored by Wall Associated Kinases: a Model. *Plant Signaling and Behavior* 10 (7):e1035854

Kohorn BD, Johansen S, Shishido A, Todorova T, Martinez R, Defeo E, Obregon P (2009) Pectin activation of MAP kinase and gene expression is WAK2 dependent. *The Plant Journal* 60 (6):974-982

Kohorn BD, Kobayashi M, Johansen S, Riese J, Huang L-F, Koch K, Fu S, Dotson A, Byers N (2006) An Arabidopsis cell wall-associated kinase required for invertase activity and cell growth. *The Plant Journal* 46 (2):307-316. doi:https://doi.org/10.1111/j.1365-313X.2006.02695.x

Kohorn BD, Kohorn SL (2012) The cell wall-associated kinases, WAKs, as pectin receptors. *Frontiers in plant science* 3 (88). doi: http://dx.doi.org/10.3389/fpls.2012.00088

Kohorn BD, Greed B, Verger S, Mouille G, Kohorn SL (2021) Effects Of Arabidopsis Wall Associated Kinase Mutations On ESMERALDA1 And Elicitor Induced ROS. *PLOS1 in press*

Kohorn BD, Zorensky FDH, Dexter-Meldrum J, Chabout S, Mouille G, Kohorn SL (2021) Mutation of an Arabidopsis Golgi Membrane Protein ELMO1 Reduces Cell Adhesion. *Development* 148 (9)

Kunudu N, Dozier U, Deslandes L, Somssich IE, Ullah H. (2013) Arabidopsis scaffold protein RACK1A interacts with diverse environmental stress and photosynthesis related proteins. *Plant Signalling & Behavior* 8 (5) DOI: 10.4161/psb.24012

Lally D, Ingmire P, Tong H-Y, He Z-H (2001) Antisense Expression of a Cell Wall–Associated Protein Kinase, WAK4, Inhibits Cell Elongation and Alters Morphology. *The Plant Cell* 13 (6):1317-1332. doi:10.1105/TPC.010075

Lim S, Jung GA, Glover DJ, Clark DS (2019) Enhanced Enzyme Activity through Scaffolding on Customizable Self-Assembling Protein Filaments. *Small* 15 (20): e1805558

Lionetti V, Cervone F, De Lorenzo G (2015) A lower content of de-methylesterified homogalacturonan improves enzymatic cell separation and isolation of mesophyll protoplasts in Arabidopsis. *Phytochemistry* 112:188-194

Lionetti V, Fabri E, De Caroli M, Hansen AR, Willats WG, Piro G, Bellincampi D (2017) Three pectin methylesterase inhibitors protect cell wall integrity for Arabidopsis immunity to Botrytis. *Plant Physiology* 173 (3):1844-1863

Lohmeier-Vogel EM, Kerk D, Nimick M, Wrobel S, Vickerman L, Muench DG, Moorhead GBG (2008) Arabidopsis At5g39790 encodes a chloroplast-localized, carbohydrate-binding, coiled-coil domain-containing putative scaffold protein. *BMC Plant Biology* 8 (120) doi: https://doi.org/10.1186/1471-2229-8-120

McCarthy TW, Der JP, Honaas LA, Claude Wd, Anderson CT (2014) Phylogenetic analysis of pectin-related gene families in Physcomitrella patens and nine other plant species yields evolutionary insights into cell walls. *BMC Plant Biology* 14 (1):1-14

Miart F, Desprez T, Biot E, Morin H, Belcram K, Höfte H, Gonneau M, Vernhettes S (2014) Spatio-temporal analysis of cellulose synthesis during cell plate formation in Arabidopsis. *The Plant Journal* 77 (1):71-84. doi:https://doi.org/10.1111/tpj.12362

Micheli F (2001) Pectin methylesterases: cell wall enzymes with important roles in plant physiology. *Trends in Plant Science* 6 (9):414-419. doi:https://doi.org/10.1016/S1360-1385(01)02045-3

Mohnen D (2008) Pectin structure and biosynthesis. *Current opinion in plant biology* 11 (3):266-277

Mouille G, Ralet MC, Cavelier C, Eland C, Effroy D, Hématy K, McCartney L, Truong HN, Gaudon V, Thibault JF (2007) Homogalacturonan synthesis in Arabidopsis thaliana

requires a Golgi-localized protein with a putative methyltransferase domain. *The Plant Journal* 50 (4):605-614
Neumetzler L, Humphrey T, Lumba S, Snyder S, Yeats TH, Usadel B, Vasilevski A, Patel J, Rose JKC, Persson S, Bonetta D (2012) The FRIABLE1 Gene Product Affects Cell Adhesion in Arabidopsis. PLOS ONE 7 (8):e42914. doi:10.1371/journal.pone.0042914
Newman RH, Hill SJ, Harris PJ (2013) Wide-angle x-ray scattering and solid-state nuclear magnetic resonance data combined to test models for cellulose microfibrils in mung bean cell walls. *Plant Physiology* 163 (4):1558-1567. doi:10.1104/pp.113.228262
Nguyen HP, Jeong HY, Jeon SH, Kim D, Lee C (2017) Rice pectin methylesterase inhibitor28 (OsPMEI28) encodes a functional PMEI and its overexpression results in a dwarf phenotype through increased pectin methylesterification levels. *Journal of Plant Physiology* 208:17-25
Nishiyama Y, Langan P, Chanzy H (2002) Crystal structure and hydrogen-bonding system in cellulose Iβ from synchrotron X-ray and neutron fiber diffraction. *Journal of the American Chemical Society* 124 (31):9074-9082
Nishiyama Y, Sugiyama J, Chanzy H, Langan PJ (2003) Crystal structure and hydrogen bonding system in cellulose Iα from synchrotron X-ray and neutron fiber diffraction. *JotACS* 125 (47):14300-14306
Nixon BT, Mansouri K, Singh A, Du J, Davis JK, Lee J-G, Slabaugh E, Vandavasi VG, O'Neill H, Roberts EM, Roberts AW, Yingling YG, Haigler CH (2016) Comparative Structural and Computational Analysis Supports Eighteen Cellulose Synthases in the Plant Cellulose Synthesis Complex. *Sci Rep* 6:28696-28696. doi:10.1038/srep28696
Pastuglia M, Roby D, Dumas C, Cock JM (1997) Rapid induction by wounding and bacterial infection of an S gene family receptor-like kinase gene in Brassica oleracea. *The Plant Cell* 9 (1):49-60
Pauly M, Gille S, Liu L, Mansoori N, de Souza A, Schultink A, Xiong G (2013) Hemicellulose biosynthesis. *Planta* 238 (4):627-642
Pauly M, Scheller HV (2000) O-Acetylation of plant cell wall polysaccharides: identification and partial characterization of a rhamnogalacturonan O-acetyl-transferase from potato suspension-cultured cells. *Planta* 210 (4):659-667
Persson S, Caffall KH, Freshour G, Hilley MT, Bauer S, Poindexter P, Hahn MG, Mohnen D, Somerville C (2007a) The Arabidopsis irregular xylem8 mutant is deficient in glucuronoxylan and homogalacturonan, which are essential for secondary cell wall integrity. *The Plant Cell* 19 (1):237-255
Persson S, Paredez A, Carroll A, Palsdottir H, Doblin M, Poindexter P, Khitrov N, Auer M, Somerville CR (2007b) Genetic evidence for three unique components in primary cell-wall cellulose synthase complexes in Arabidopsis. *PNAS* 104 (39):15566-15571. doi:10.1073/pnas.0706592104
Rautengarten C, Birdseye D, Pattathil S, McFarlane HE, Saez-Aguayo S, Orellana A, Persson S, Hahn MG, Scheller HV, Heazlewood JL, Ebert B (2017) The elaborate route for UDP-arabinose delivery into the Golgi of plants. *Proceedings of the National Academy of Sciences* 114 (16):4261-4266. doi:10.1073/pnas.1701894114
Ren C, Kermode AR (2000) An increase in pectin methyl esterase activity accompanies dormancy breakage and germination of yellow cedar seeds. *Plant Physiology* 124 (1):231-242

Rhee SY, Osborne E, Poindexter PD, Somerville CR (2003) Microspore separation in the quartet 3 mutants of Arabidopsis is impaired by a defect in a developmentally regulated polygalacturonase required for pollen mother cell wall degradation. *Plant Physiology* 133 (3):1170-1180
Ridley BL, O'Neill MA, Mohnen D (2001) Pectins: structure, biosynthesis, and oligogalacturonide-related signaling. *Phytochemistry* 57 (6):929-967
Robert HS, Quint A, Brand Q, Vivian-Smith A, Offringa R (2009) BTB and TAZ domain scaffold proteins perform a crucial function in Arabidopsis development. *The Plant Journal* 58 (1):109-121. doi: https://doi.org/10.1111/j.1365-313X.2008.03764.x
Rocchi V, Janni M, Bellincampi D, Giardina T, D'ovidio R (2012) Intron retention regulates the expression of pectin methyl esterase inhibitor (Pmei) genes during wheat growth and development. *Plant Biology* 14 (2):365-373
Röckel N, Wolf S, Kost B, Rausch T, Greiner S (2008) Elaborate spatial patterning of cell-wall PME and PMEI at the pollen tube tip involves PMEI endocytosis, and reflects the distribution of esterified and de-esterified pectins. *The Plant Journal* 53 (1):133-143
Scheible W-R, Eshed R, Richmond T, Delmer D, Somerville C (2001) Modifications of cellulose synthase confer resistance to isoxaben and thiazolidinone herbicides in Arabidopsis Ixr1 mutants. *Proceedings of the National Academy of Sciences* 98 (18):10079-10084
Scheller HV, Ulvskov P (2010) Hemicelluloses. Annual review of plant biology 61
Srivastava S, Gupta SM, Sane AP, Nath P (2012) Isolation and characterization of ripening related pectin methylesterase inhibitor gene from banana fruit. Physiology Molecular *Biology of Plants* 18 (2):191-195
Suslov D, Verbelen J (2006) Cellulose orientation determines mechanical anisotropy in onion epidermis cell walls. *Journal of Experimental Botany* 57 (10):2183-2192
Takasaki T, Hatakeyama K, Suzuki G, Watanabe M, Isogai A, Hinata K (2000) The S receptor kinase determines self-incompatibility in Brassica stigma. *Nature* 403 (6772):913-916
Tetlow IJ, Beisel KG, Cameron S, Makhmoudova A, Liu F, Bresolin NS, Wait R, Morell MK, Emes MJ (2008) Analysis of Protein Complexes in Wheat Amyloplasts Reveals Functional Interactions among Starch Biosynthetic Enzymes. *Plant Physiology* 146:1878-1891 doi:https://doi.org/10.1104/pp.108.116244
Tian G-W, Chen M-H, Zaltsman A, Citovsky V (2006) Pollen-specific pectin methylesterase involved in pollen tube growth. *Developmental Biology* 294 (1):83-91
Tieman DM, Handa AK (1994) Reduction in pectin methylesterase activity modifies tissue integrity and cation levels in ripening tomato (Lycopersicon esculentum Mill.) fruits. *Plant Physiology* 106 (2):429-436
Toyooka K, Goto Y, Asatsuma S, Koizumi M, Mitsui T, Matsuoka K (2009) A mobile secretory vesicle cluster involved in mass transport from the Golgi to the plant cell exterior. *The Plant Cell* 21 (4):1212-1229
van Oostende-Triplet C, Guillet D, Triplet T, Pandzic E, Wiseman PW, Geitmann A (2017) Vesicle Dynamics during Plant Cell Cytokinesis Reveals Distinct Developmental Phases. *Plant Physiology* 174 (3):1544-1558. doi:10.1104/pp.17.00343
Van Sandt VS, Suslov D, Verbelen J-P, Vissenberg K (2007) Xyloglucan endotransglucosylase activity loosens a plant cell wall. *Annals of Botany* 100 (7):1467-1473
Vandavasi VG, Putnam DK, Zhang Q, Petridis L, Heller WT, Nixon BT, Haigler CH, Kalluri U, Coates L, Langan P, Smith JC, Meiler J, O'Neill H (2016) A Structural Study of CESA1

Catalytic Domain of Arabidopsis Cellulose Synthesis Complex: Evidence for CESA Trimers. *Plant Physiology* 170 (1):123-135. doi:10.1104/pp.15.01356

Verger S, Chabout S, Gineau E, Mouille G (2016) Cell adhesion in plants is under the control of putative O-fucosyltransferases. *Development* 143 (14):2536-2540. doi:10.1242/dev.132308

Wagner TA, Kohorn BD (2001) Wall-associated kinases are expressed throughout plant development and are required for cell expansion. *The Plant Cell* 13 (2):303-318

Wang Y, Shao L, Shi S, Harris RJ, Spellman MW, Stanley P, Haltiwanger RS (2001) Modification of epidermal growth factor-like repeats with O-fucose: molecular cloning and expression of a novel GDP-fucose proteinO-fucosyltransferase. *J Journal of Biological Chemistry* 276 (43):40338-40345

Wen F, Zhu Y, Hawes MC (1999) Effect of pectin methylesterase gene expression on pea root development. *The Plant Cell* 11 (6):1129-1140

Willats WGT, McCartney L, Steele-King CG, Marcus SE, Mort A, Huisman M, van Alebeek G-J, Schols HA, Voragen AGJ, Le Goff A, Bonnin E, Thibault J-F, Knox JP (2004) A xylogalacturonan epitope is specifically associated with plant cell detachment. *Planta* 218 (4):673-681. doi:10.1007/s00425-003-1147-8

Zamil MS, Geitmann A (2017) The middle lamella-more than a glue. *Physical Biology* 14 (1):015004. doi:10.1088/1478-3975/aa5ba5

Zhu C, Ganguly A, Baskin TI, McClosky DD, Anderson CT, Foster C, Meunier KA, Okamoto R, Berg H, Dixit R (2015) The fragile Fiber1 kinesin contributes to cortical microtubule-mediated trafficking of cell wall components. *Plant Physiology* 167 (3):780-792

Zykwinska AW, Ralet M-CJ, Garnier CD, Thibault J-FJ (2005) Evidence for in vitro binding of pectin side chains to cellulose. *Plant Physiology* 139 (1):397-407